Studies on Electrode Processes of Stabilized Zirconia Cell System by Complex Impedance Method

Jun SASAKI,* Junichiro MIZUSAKI, Shigeru YAMAUCHI, and Kazuo FUEKI

Department of Industrial Chemistry, Faculty of Engineering, The University of Tokyo, Hongo, Bunkyo-ku, Tokyo 113

(Received November 20, 1980)

Three kinds of materials, Pt, Ag, and $La_{0.5}Sr_{0.5}CoO_3$, were applied to stabilized zirconia as electrodes and the electrode behavior was investigated by means of the complex impedance method. The impedance arc due to the electrode/stabilized zirconia interface was always depressed semi-circles. Impedance behavior was strongly dependent on the electrode materials. Assuming that the impedance arc could be interpreted by a parallel *R-C* circuit, the interface resistance R_i and the interface capacitance C_i were determined. The apparent activation energy determined from the slope of the plots of log R_i *vs.* $1/T$ was nearly the same for the same electrode material. (Ag electrode: 92 kJ/mol and Pt electrode: 201 kJ/mol). The oxygen pressure dependence of C_i and R_i was also investigated. Although C_i was virtually independent of the oxygen partial pressure P_{O_2}, R_i was proportional to $P_{O_2}^{-2/3}$ for Ag electrodes and $P_{O_2}^{-1/4}$ for Pt electrodes. The rate-determining step was supposed to be the dissociation of oxygen molecules into atoms for Ag electrodes, and the dissociation of oxygen molecules or one of the subsequent steps for Pt electrodes.

The complex impedance method has been widely used to study the solid state cell systems.[1-8] This method provides an important tool for separating the impedance due to interfacial phenomena from that due to bulk properties of solid state cells.

So far, a lot of works have been carried out by this method to investigate the polarization processes at the stabilized zirconia/electrode interface.[1-7] However, results by different investigators were often inconsistent. This would be partly due to the scarcity of experimental evidence on the relationship between the interface behavior and electrode materials.

The purpose of the present study is to elucidate the influences of the nature of electrode materials on the polarization process by the complex impedance method.

Experimental

The electrolyte used in the experiments was 8 m/o yttria-stabilized zirconia disks supplied by Toray Industries, Inc. The diameter of the sample was 10 mm. Three different thickness, 1, 5, and 10 mm, were used in order to separate bulk properties from the interfacial ones of the stabilized zirconia cell. Both faces of stabilized zirconia disk were polished with No. 2000 emery paper and rinsed with alkaline cleaning solution.

The electrodes were prepared in various ways. Three kinds of electrode materials, Pt, Ag, and $La_{0.5}Sr_{0.5}CoO_3$ were applied to both faces of stabilized zirconia disks. The methods of preparation are listed in Table 1. Sputtered electrodes were prepared by means of RF sputtering (1500 V, 5×10^{-2} Torr† argon, 10—180 min) from a nominally pure foil of Pt or Ag. Evaporation was carried out by means of the electron beam melting furnace. Pt electrodes from H_2PtCl_6 were obtained by repeated application of H_2PtCl_6 aqueous solution subsequently followed by firing to drive off H_2O and Cl_2 gas. Pastes with glass flux were commercial materials from Tanaka-Matthey (Pt paste: 760A, Ag paste: FSP-306). Platinum paste without glass flux were prepared using Pt powder and an organic suspending medium. $La_{0.5}Sr_{0.5}CoO_3$ was prepared by mixing $La_2(CO_3)_3$, $SrCO_3$ and $CoCO_3$, and firing the mixture at 1100 °C for 8 h. $La_{0.5}Sr_{0.5}CoO_3$ thus obtained was then ground into powder and mixed with organic suspending medium. Then the paste of $La_{0.5}Sr_{0.5}CoO_3$ was applied on both faces of stabilized zirconia. Platinum gauze (200 mesh-cm^{-1}) connected with a Pt lead wire was dipped into the $La_{0.5}Sr_{0.5}CoO_3$ paste. Then, the paste was dried and fired at 1200 °C for 12 h. As current collectors, Ag gauze was used for Ag electrodes and Pt gauze for other electrodes. The gauze was pressed to electrodes by two very porous alumina disks to make sure the good contact.

Table 1. Electrode materials and method of preparation

Electrode material	Method of preparation
Platinum	Sputtering
	Evaporation
	Decomposition of H_2PtCl_6
	Paste with glass flux
	Paste without glass flux
Silver	Paste with glass flux
	Sputtering
$La_{0.5}Sr_{0.5}CoO_3$	Paste without glass flux

Measurements were made in the temperature ranges, 500—900 °C for the cells with Pt electrodes, 350—800 °C for those with Ag electrodes and 400—1200 °C for those with $La_{0.5}Sr_{0.5}CoO_3$ electrodes.

The complex impedance measurements were performed over the frequency range of 20 kHz to 5 Hz by means of a phase sensitive detector (Complex Impedance Meter 7010, Toho Technical Research Co.). In the frequency range from 1 Hz to 0.001 Hz Lissajous figure method was used. In this method the sine wave voltage was applied to the combination of the cell and a standard resistance in series by a sine wave generator (WAVETEK Model 184). The input and output signals were displayed simultaniously on an X-Y recorder, and the impedance of the cell was determined from the dimensions of Lissajous figures. The oxygen partial pressure (1—10^{-4} atm) was controlled by mixing oxygen and pure argon gas.

Results and Discussion

Effects of Electrode Materials on Interface Impedance.

Pt Electrode: Figure 1 gives the impedance plots of the specimens with various types of Pt electrodes measured

† 1 Torr = 133.322 Pa.

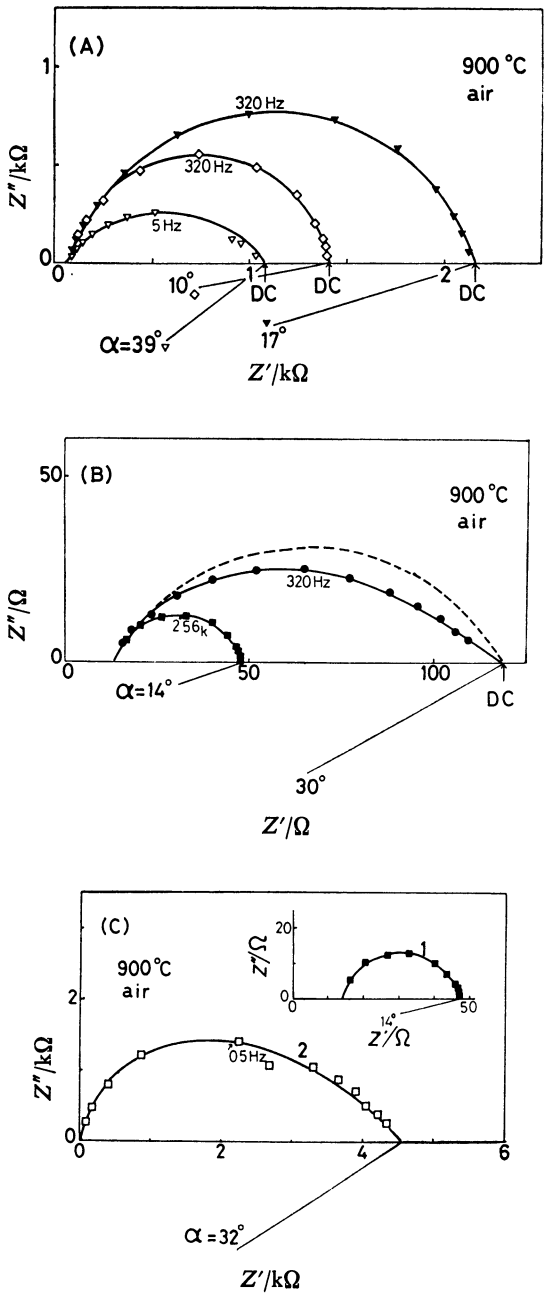

Fig. 1. Impedance plots of the cell with Pt electrodes. (A): ▼; evaporated Pt, ◇; sputtered Pt, ▽; Pt from H_2PtCl_6. (B): ●; Pt paste with glass flux, ■; Pt paste without glass flux. (C): Pt paste without glass flux, ■; before annealing at 1300 °C for 72 h, □; after annealing at 1300 °C for 72 h.

in air. Stabilized zirconia disks used were 5 mm in thickness. The semi-circular arc corresponds to the impedance at the electrode/stabilized zirconia interface. Figure 1(A) shows the impedance plots of specimens with Pt electrodes from evaporation, sputtering or decomposition of H_2PtCl_6. The centers of semi-circles are not on the real axis. Therefore, the results cannot be fully interpreted by an equivalent circuit of a parallel *R-C* combination. The depression angle α represents the deviation of the center of circle from the real axis. Two intercepts of the arc with the real axis give the resistivity of the equivalent circuit of the interface impedance.[1,2,10] The difference R_i between these intercepts is the sum of the interface resistances at cathode and anode. In the present study, the voltage applied to the electrode was kept below 10 mV in order to avoid non-linearity between the current and the overvoltage, and the polarization resistances at both electrodes are therefore supposed to be equal.

Figure 1(B) gives the impedance plots of specimens with Pt paste electrodes with or without glass flux. It is evident that glass flux depresses the impedance arc, especially in the right side of arc, which means that the curvature of arc in the low frequency region is smaller than that in the high frequency region.

Figure 1 (C) shows the effects of the annealing on the impedance plots for the specimen with Pt paste electrode without glass flux. Platinum paste without glass flux was applied on the faces of stabilized zirconia and fired at 900 °C for 3 h and then at 1300 °C for 72 h. Curves 1 and 2 in the figure were impedance arcs measured before and after the annealing at 1300 °C respectively. It is apparent from the figure that the long period annealing has resulted in a noticeable increase in interface resistance and a depression of semi-circle. This may be due to the decrease in the three phase boundary (lines where the electrode, electrolyte and gas phase meet) and the decrease in the interconnected gas channels in the Pt electrode. So far, the depression of impedance arc has been accounted for by the contribution of Warburg impedance.[2] The decrease in the volume of open pores in electrode accompanies the decrease in diffusion flux of gaseous species. Accordingly, the contribution of Warburg impedance to the interface impedance increases. Likewise, the addition of glass flux is supposed to decrease the diffusion flux and to cause the increase in the depression angle.

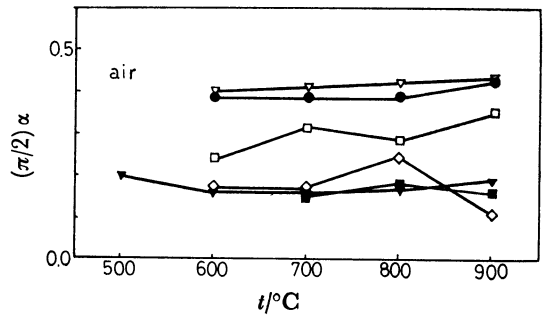

Fig. 2. Temperature dependence of α.
▽: Pt from H_2PtCl_6, ●: Pt paste with glass flux, □: Pt paste without glass flux annealed at 1300 °C for 72 h, ◇: sputtered Pt, ▼: evaporated Pt, ■: Pt paste without glass flux.

Figure 2 shows the depression angle α against temperature for various types of Pt electrodes in air. The electrodes with relatively thin films, for example the sputtered or evaporated electrodes, seem to have somewhat small depression angle. But in the case of Pt paste electrodes with glass flux, correlation was not observed between the electrode thickness and the depression angle.

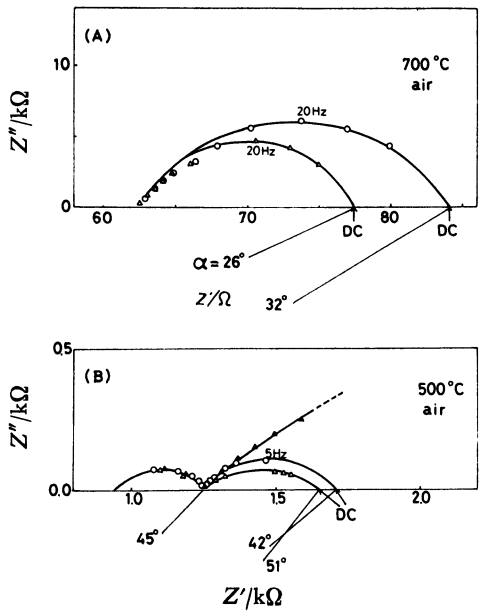

Fig. 3. Impedance plots of the cell with Ag and $La_{0.5}Sr_{0.5}CoO_3$ electrodes.
○: Ag paste with glass flux, △: sputtered Ag, ▲: $La_{0.5}Sr_{0.5}CoO_3$.

Ag Electrode: Figure 3 shows the impedance plots of the cells with Ag electrodes and $La_{0.5}Sr_{0.5}CoO_3$ electrode measured in air. Stabilized zirconia disks used were 5 mm in thickness. Although only one arc was observed at high temperature (above 550 °C), below 550 °C the second arc appeared in the high frequency region for both Ag and $La_{0.5}Sr_{0.5}CoO_3$ electrodes. Impedance measurements on specimens with different thickness of electrolyte showed that the high frequency dispersion is dependent on the electrolyte thickness but independent of the method of preparation of Ag electrodes. Accordingly, the arc of high frequency region would corresponds to the impedance of grain boundary.[1-8]

The arc in the low frequency region would corresponds to the interface impedance. Silver electrodes prepared from Ag paste with glass flux gave a more depressed arc in the low frequency region than the sputtered one at temperatures below 500 °C. In the case of Ag and $La_{0.5}Sr_{0.5}CoO_3$ electrodes, the interface resistance R_i is given from the two intercepts of impedance arc with the real axis in the low frequency region.

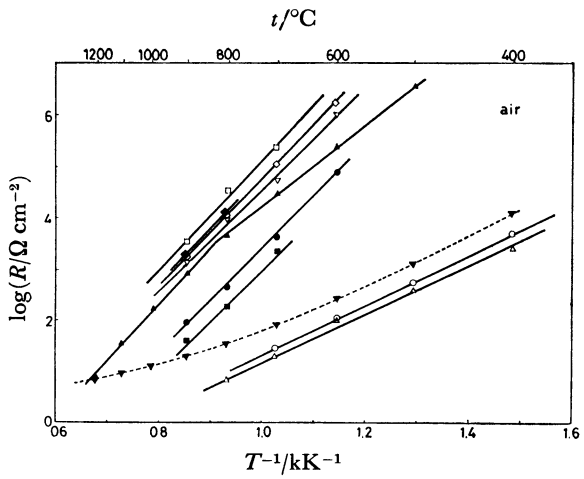

Fig. 4. Plots of log R_i *vs.* $1/T$.
□: Pt paste without glass flux annealed at 1300 °C for 72 h, ◇: sputtered Pt, ◆: evaporated Pt, ▽: Pt from H_2PtCl_6, ▲: $La_{0.5}Sr_{0.5}CoO_3$, ●: Pt paste with glass flux, ■: Pt paste without glass flux, ○: Ag paste with glass flux, △: sputtered Ag.

Figure 4 shows the plots of log R_i against $1/T$ for various kinds of electrodes. The broken line indicates the bulk resistance of stabilized zirconia measured in this study. Since the grain boundary impedance is negligible above 550 °C, the bulk resistance is determined from the intercept of the impedance arc with the real axis at high frequency region. When the grain boundary impedance arc appears below 550 °C, the bulk resistance is determined from the extrapolation to high frequency in the grain boundary region.[2] As can be seen from the figure, Ag electrodes have relatively low interface resistance. $La_{0.5}Sr_{0.5}CoO_3$ is a mixed conductor which has high ionic conductivity as well as high electronic conductivity.[9] So, it is expected that oxygen dissolves into the oxide electrode and is ionized at the electrode/electrolyte interface. This means that the reaction area is much larger than that of three phase boundary. But, the experimental results did not show any evidence of low interface resistance.

From Fig. 4, it is evident that the same metal has nearly the same activation energy. This fact suggests that the rate-determining step of the electrode processes is the same for the same metal in a temperature range studied. It was found that the activation energy for Pt electrodes is about 201 kJ/mol and that for Ag electrodes is about 92 kJ/mol.

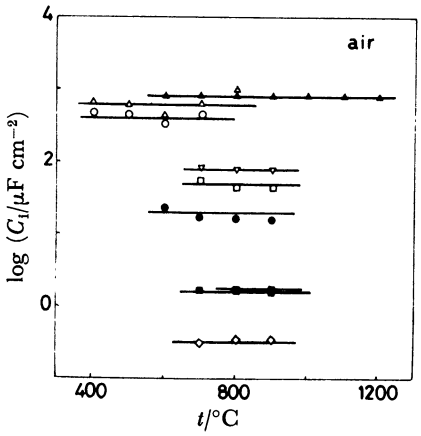

Fig. 5. Temperature dependence of log C_i.
▲: $La_{0.5}Sr_{0.5}CoO_3$, △: sputtered Ag, ○: Ag paste with glass flux, ▽: Pt from H_2PtCl_6, □: Pt paste without glass flux annealed at 1300 °C for 72 h, ●: Pt paste with glass flux, ▼: evaporated Pt, ■: Pt paste without glass flux, ◇: sputtered Pt.

Figure 5 shows log C_i against temperature for various kinds of electrode materials, where C_i is the interface capacitance calculated from the impedance plots assuming that the interface impedance is approximated by *R-C* parallel circuit. It is obvious that the interface capacitance is independent of the temperature and strongly dependent on the preparation of electrode.

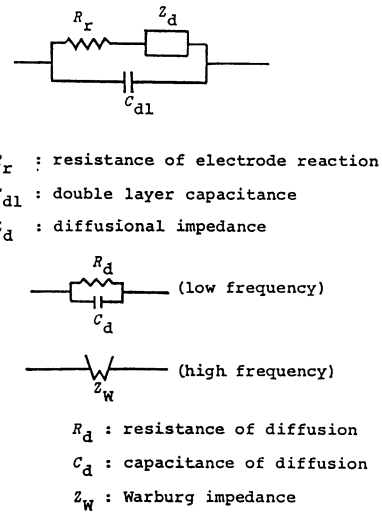

Fig. 6. Equivalent circuit of interface impedance.

Sputtered or evaporated Pt electrodes show small capacitance. Since C_i is considered to be proportional to the contact area at the electrode material/electrolyte interface, the small capacitance would be explained as the low contact area.

Equivalent Circuit and Oxygen Pressure Dependence of the Interface Impedance. As shown in Figs. 1 and 3, the impedance arcs for various kinds of electrodes are depressed. Therefore they cannot be accounted for by a parallel R-C combination.

According to Franklin,[10] when the gas diffusion in pores of electrode is slow, the equivalent circuit is as shown in Fig. 6. In this equivalent circuit, Z_d expresses the impedance due to diffusional process of gaseous oxygen in pores, which is approximated by Warburg impedance in the high frequency region and by a parallel R_d-C_d circuit in the low frequency region. Accordingly, the interface resistance is represented by the sum of the diffusional resistance R_d and the electrode reaction resistance R_r. Therefore, the higher one of R_d and R_r determines the interface resistance. Since R_d is proportional to $1/P_{O_2}$ and C_d is proportional to P_{O_2}, the P_{O_2} dependence of the impedance plots elucidate the contribution of R_d and C_d.

Figure 7 gives the change in the impedance plots with oxygen pressure for specimens with Pt electrode from H_2PtCl_6 and sputtered Ag electrode. The interface resistance R_i increases as the P_{O_2} decreases. However, the capacitance obtained by assuming the parallel R-C circuit was found to be independent of the P_{O_2} as shown in Fig. 8. Probably, the capacitance would correspond to the double layer capacitance in Fig. 6.

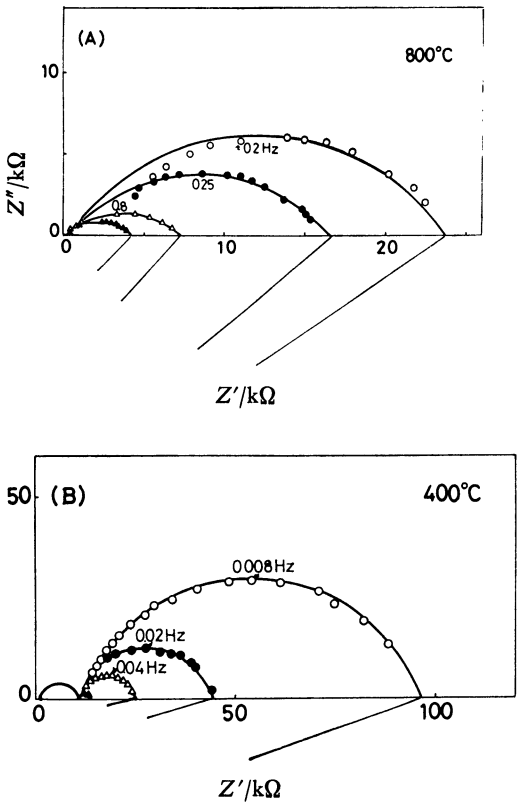

Fig. 7. P_{O_2} dependence of impedance plot.
(A): Pt from H_2PtCl_6. P_{O_2}/atm ▲; 1.0, △; 2.0×10^{-1}, ●; 1.1×10^{-2}, ○; 8.5×10^{-4}. (B): sputtered Ag P_{O_2}/atm ▲; 3.0×10^{-2}, △; 1.1×10^{-2}, ●; 2.1×10^{-3}, ○; 6.5×10^{-4}.

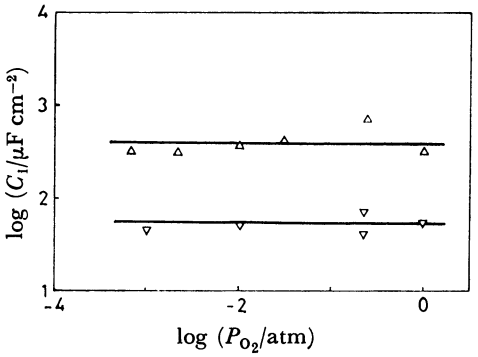

Fig. 8. P_{O_2} dependence of log C_i.
△: Sputtered Ag (400 °C), ▽: Pt from H_2PtCl_6 (800 °C).

Figure 9 (A) shows the P_{O_2} dependence of the interface resistance of Pt electrodes. The interface resistance is proportional to $P_{O_2}^{-1/4}$, irrespective of electrode preparation. Bauerle's[1] results on sputtered Pt electrodes show a tendency of saturation with the increase in P_{O_2}.

Figure 9 (B) shows the same plot for the sputtered Ag electrode. The interface resistance is proportional to $P_{O_2}^{-2/3}$.

From the results shown in Fig. 9, under low overvoltages the interface resistance of both Pt and Ag electrode is attributed to the resistance of electrode reaction R_r in Fig. 6.

Electrode Reaction. As indicated in the preceding section, the interface impedance can be approximated by the parallel R_r(resistance of electrode reaction)-C_{dl} (double layer capacitance) circuit in spite of the depression of the impedance arcs. Unlike C_{dl}, R_r was found to be sensitive to temperature and oxygen pressure. One may consider $1/R_r$ to be a measure of the rate of over-all electrode reaction. The over-all electrode reaction consists of several elementary steps given in Table 2. The value of n in the form of $1/R_r \propto P_{O_2}^n$,

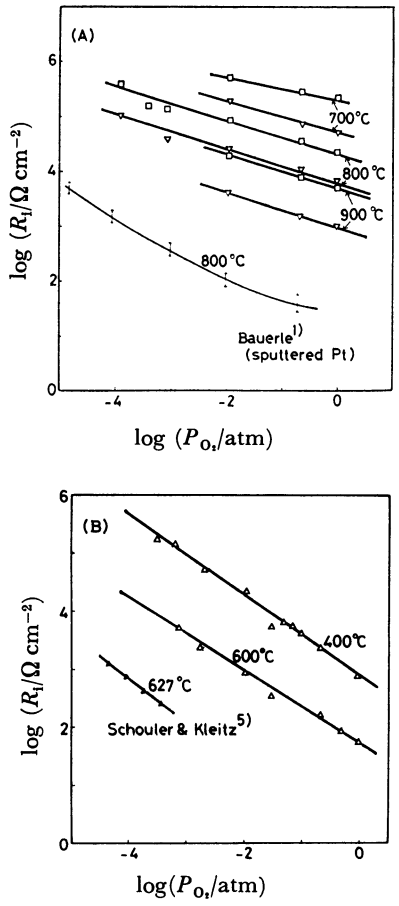

Fig. 9. P_{O_2} dependence of log R_i.
(A): □; Pt paste without glass flux annealed at 1300 °C for 72 h, ▽; Pt from H_2PtCl_6. (B): Sputtered Ag.

characteristic of each rate-determining step is also given in Table 2. If step (I) is rate-determining, $1/R_r$ should be proportional to P_{O_2} ($n=1$). From the results obtained in this work, $1/R_r$ is not proportional to P_{O_2}. So, this adsorption process is considered to be not rate-determining. When the step (II) is rate-determining and the adsorption of oxygen obeys Langmuir isotherm, n is supposed to take values from 1 to 0. Similarly, n would take values from 1/2 to 0, when step (III) or (IV) is rate-determining. Results of the present work indicate that n is 2/3 for Ag electrodes. Moreover, Buttner and his co-investigators[11)] have found that

TABLE 2. ELEMENTARY REACTION STEPS AND THE VALUE OF n, CHARACTERISTIC OF RATE-DETERMINING STEP

	Elementary step	n in $1/R_r \propto P_{O_2}^n$
I	$O_2(g) \rightleftarrows O_2$ (ad)	1
II	$O_2(ad) \rightleftarrows 2O$ (ad)	1—0
III	Surface diffusion of O(ad)	1/2—0
IV	$O(ad)+2e \rightleftarrows O^{2-}$	1/2—0

oxygen is strongly adsorbed on the surface of Ag. From these results, the rate-determining step of the electrode processes on Ag electrodes is supposed to be the dissociation of adsorbed oxygen molecules into atoms.

For Pt electrodes, n was found to be 1/4. According to Fryburg and Petrus,[12)] at temperatures and oxygen pressure studied, the surface of Pt would be completely covered with a tightly bound monolayer of oxygen atoms. So, we could assume the weakly adsorbed molecular oxygen. If the adsorption is Langmuir type, the rate-determining step would be the dissociation of oxygen molecules into atoms or either one of the subsequent steps.

References

1) J. E. Bauerle, *J. Phys. Chem. Solids*, **30**, 2657 (1969).
2) Y. Suzuki and T. Takahashi, *Denki Kagaku*, **39**, 406 (1971).
3) E. Schouler, M. Kleitz, and C. Deportes, *J. Chim. Phys.*, **70**, 923 (1973).
4) E. Schouler, G. Giroud, and M. Kleitz, *J. Chim. Phys.*, **70**, 1309 (1973).
5) E. Schouler and M. Kleitz, *J. Electroanal. Chem. Interfacial Electrochem.*, **64**, 135 (1975).
6) N. Matsui, *Surf. Sci.*, **86**, 353 (1979).
7) P. Fabry, E. Schouler, and M. Kleitz, *Electrochim. Acta*, **23**, 539 (1978).
8) S. H. Chu and M. A. Seitz, *J. Solid State Chem.*, **23**, 297 (1978).
9) H. Obayashi and T. Kudo, "Application of Solid Electrolytes," ed by T. Takahashi and A. Kozawa, JEC Press, Ohio, U.S.A. (1980), p. 106.
10) A. D. Franklin, *J. Am. Ceram. Soc.*, **58**, 465 (1975).
11) F. H. Buttner, E. R. Funk, and H. Udin, *J. Phys. Chem.*, **56**, 657 (1952).
12) G. C. Fryburg and H. M. Petrus, *J. Electrochem. Soc.*, **108**, 496 (1961).